Theoretical Investigation of Substrate Effect on Deliquescence Relative Humidity of NaCl Particles

Yonggang Gao, Liya E. Yu,† and Shing Bor Chen*

Department of Chemical and Biomolecular Engineering, National University of Singapore, Singapore 117576

Received: August 24, 2006; In Final Form: October 23, 2006

A theoretical investigation is conducted for the first time to explore the deliquescence of particles deposited on a substrate. The formulation incorporates the Kelvin effect with the assumption that the dry and wet particles are both spherical caps in shape. Unlike the deposited particles larger than 500 nm, the deliquescence relative humidity (DRH) of smaller particles can substantially depend on the particle size, the contact angles, and the surface tension between the particle and the atmosphere. At certain contact angles, small particles depositing on a substrate could deliquesce at a much lower RH, posing a potential corrosion problem for metallic substrates.

1. Introduction

The hygroscopic properties of airborne particles have received increasing attention because of the subsequent effects on atmospheric visibility and earth's climate.[1−4] Whereas most studies examined the water sorption of suspended particles,[3,5−10] little effort has been devoted to investigating the hygroscopic behavior of particles deposited on a substrate. The hygroscopicity of deposited particles is important because substantial water sorption can lead to surface corrosion, a serious problem for electronic devices (such as printed circuit boards)[11−13] in contact with potentially corrosive particles.[11,12,14,15] Therefore, to minimize costly failure in the usage of electronics, it is necessary to understand the hygroscopicity of deposited particles.

Table 1 shows the limited available experimental works investigating $(NH_4)_2SO_4$ and NaCl particles on three types of substrates.[16,17] The resultant deliquescence relative humidities (DRH) of deposited particles with sizes ranging from 0.1 to 20 μm are between 75% RH and 80% RH (Table 1), consistent with the DRH of suspended micron-size $(NH_4)_2SO_4$ and NaCl particles.[18−21] Therefore, the substrates appear to have a very weak effect on the hygroscopicity of deposited particles. This result can be attributed to the large particle sizes examined in the studies because both experimental observations (Table 2) and theoretical simulation for suspended NaCl particles[22] consistently show an increase of DRH with the decreasing particle size for particles smaller than 60 nm. Hence, for small deposited particles, we also expect a noticeable size effect on deliquescence.

For suspended particles, Mirabel et al.[23] made a theoretical prediction for DRH by equalizing the free energies for a dry particle and a droplet, in which the solid has completely dissolved. This approach was later modified by Russell and Ming,[22] who allowed for a thin water layer coated on the particle, replacing the aforementioned dry state. The wetted particle was handled under the capillarity approximation. A more thermodynamically rigorous theory was formulated by Djikaev et al.[24] This two-dimensional model calculated the free energy of a composite particle consisting of a partly dissolved solid core and a surrounding solution shell. Treating the radii of the solid core and the composite particle as two independent variables, the authors were able to draw a contour plot for the free energy at a given relative humidity and determine the equilibrium path from a dry particle to a droplet. The important findings are as follows: (1) deliquescence is not prompt[7] when RH is not high enough, reflected by a metastable coated particle having a local minimum of free energy along the path, corresponding to the initial water uptake; (2) a dramatic particle growth associated with complete dissolution can occur, provided that the droplet state has a lower free energy than the uncoated state and the metastable state, and the energy barrier can be

TABLE 1: Available Experimental DRHs of Deposited $(NH_4)_2SO_4$ and NaCl Particles

particle size (μm)	materials	substrates	DRH(%)	methods	ref
0.1−20[a]	$(NH_4)_2SO_4$	stainless steel	79.8 ± 1.5	ESEM[b]	16
	NaCl		77.5 ± 1.3		
0.1−4[a]	$(NH_4)_2SO_4$	carbon, Formvar/ carbon type TEM grid	80−81	ETEM[c]	17
	NaCl		75−77		

[a] Reported in refs 16 and 17. [b] Environmental scanning electron microscope. [c] Environmental transmission electron microscope.

TABLE 2: DRHs of Suspended NaCl Particles in Nanometer Size

particle size (nm)	materials	DRH(%)	methods	ref
8	NaCl	80.9 ± 2	UF-DMA[a]	21
10		82.4 ± 2		
15		81.3 ± 2		
30		75.6 ± 1		
50		76.0 ± 1		
6	NaCl	87 ± 2.5	TnDMA[b]	10
8		84 ± 2.5		
15		80 ± 2.5		
20		(77−78) ± 2.5		
30		77 ± 2.5		
60		(76−77) ± 2.5		

[a] Ultrafine tandem differential mobility analyzer. [b] Tandem nanodifferential mobility analyzer.

* To whom correspondence should be addressed. E-mail: checsb@nus.edu.sg.

† Division of Environmental Science & Engineering, NUS, Singapore.

10.1021/jp0654967 CCC: $37.00
Published on Web 01/09/2007

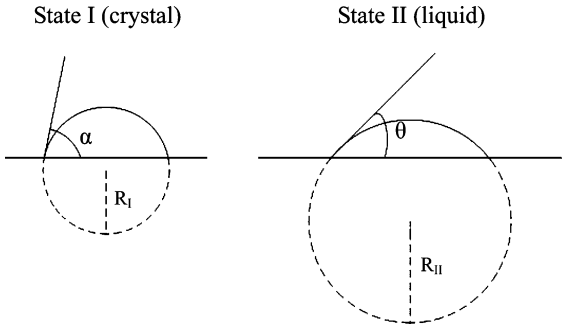

Figure 1. Schematic of a deposited particle on a substrate before and after deliquescence.

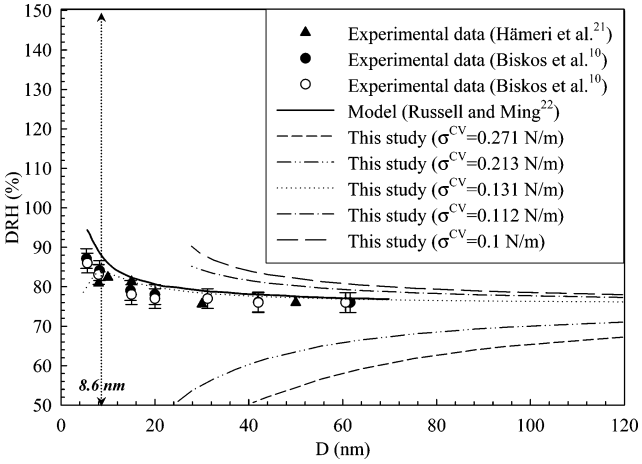

Figure 2. Effect of surface tension on the DRH of suspended NaCl particles. The prediction is compared with experimental data of Biskos et al.[10] and Hämeri et al.[21] and with the model of Russell and Ming.[22]

overcome; (3) at sufficiently high RH, the energy barrier and the metastable state both disappear, and the deliquescence becomes prompt; (4) hysteresis is predictable for the reverse process (efflorescence). Quantitative agreement between theory and experiment depends greatly on the accuracy of physical parameters, such as surface tension, activities, etc. The predicted metastable composite particle can justify the use of a wetted particle in the work of Russell and Ming, but their equalization of free energies would, in principle, underpredict DRH. Nevertheless, acceptably good agreement with DRH experiment has been achieved by using appropriate values of surface tension.[22] In fact, the method of Mirabel et al.[23] becomes equivalent to that of Russell and Ming, when an "effective" surface tension between solid and vapor is adopted instead. More detailed arguments will be given later in section 3.

Up to now, all of the available thermodynamic models are applicable to predict the DRH only for suspended particles.[22−24] The present study, for the first time, examines the trend in DRH of deposited particles. The DRH in the present study is defined as the relative humidity at which a dramatic increase in particle size takes place. In view of methodology simplicity and qualitative elucidation, we extend the theory of Mirabel et al.[23] with the assumptions that both the particle and droplet are spherical caps in shape, having different contact angles from the substrate. Because of scarce experimental data for verification of this theoretical work, we also suggest possible experimental techniques and measurements as a future work.

2. Deliquescence of a Deposited Particle

According to the Wulff theorem, the shape of a crystal on a substrate depends on the wetting condition: no wetting, imperfect wetting, or perfect wetting.[25,26] To facilitate the theoretical formulation, we assume that a deposited solid particle exhibits the shape of a spherical cap satisfying Young's equation, analogous to a droplet on a substrate. The advantage of this assumption is that it is unnecessary to know the surface tension between the particle and the substrate, as will be shown in the following derivation. Although a spherical cap can represent the shape of a nucleus formed on a substrate,[2,27−31] we state that the shape of a particle depends on the deposition process and does affect DRH.

Figure 1 shows the schematic of a deposited particle before (state I) and after (state II) deliquescence, where α and θ are the contact angles and R_I and R_{II} are the curvature radii for the two states. The free energies of the two states are expressed respectively as

$$G_I = N\mu_1^V + n_2\mu_2^C + \sigma^{CV}a^{CV} + \sigma^{CS}a^{CS} + \sigma^{SV}(S - a^{CS}) \quad (1)$$

$$G_{II} = n_1\mu_1 + n_2\mu_2 + (N - n_1)\mu_1^V + \sigma^{LV}a^{LV} + \sigma^{LS}a^{LS} + \sigma^{SV}(S - a^{LS}) \quad (2)$$

where N is the number of water molecules in the vapor of state I; n_1 is the number of water molecules in solution; n_2 is the number of the salt molecules; μ_1^V is the chemical potential of water vapor; μ_2^C is the chemical potential of solid crystal; μ_1 is the chemical potential of water in solution; μ_2 is the chemical potential of solute in solution; S is the surface area of substrate; σ^{ij} denotes the interfacial tension between phase i and j, which can be L (droplet), V (gas), S (substrate), or C (crystal). For a spherical cap with contact angle β and curvature radius R, its volume and surfaces areas are given by

$$V = \frac{1}{3}\pi R^3(1 - \cos\beta)^2(2 + \cos\beta) \quad (3)$$

$$a^{iV} = 2\pi R^2(1 - \cos\beta) \quad (4)$$

$$a^{iS} = \pi R^2 \sin^2\beta \quad (5)$$

where i can be L or C. The relation among the interfacial tensions is described by Young's equation:

$$\sigma^{SV} = \sigma^{CS} + \sigma^{CV}\cos\alpha = \sigma^{LS} + \sigma^{LV}\cos\theta \quad (6)$$

The chemical potentials for different species are expressed by

$$\mu_1 = \mu_1^0 + kT\ln a_1 \quad (7)$$

$$\mu_1^V = \mu_1^0 + kT\ln\frac{p}{p_\infty^0} \quad (8)$$

$$\mu_2 = \mu_2^C + kT\,n\frac{a_2}{\bar{a}_2} \quad (9)$$

where a_1 and a_2 are the water and the solute activity in the droplet; $\bar{a}_2$ is the solute activity in a bulk saturated solution; p is the water vapor pressure with p_0^∞ being the corresponding saturation value; kT is the themal energy. The volumes of the crystal and droplet can be related to the molecular volumes as n_2v^c and $n_1v_1 + n_2v_2$, where v^c is the molecular volume of solid crystal; v_1 and v_2 are the partial molecular volume of water and solute in the solution, respectively.[23]

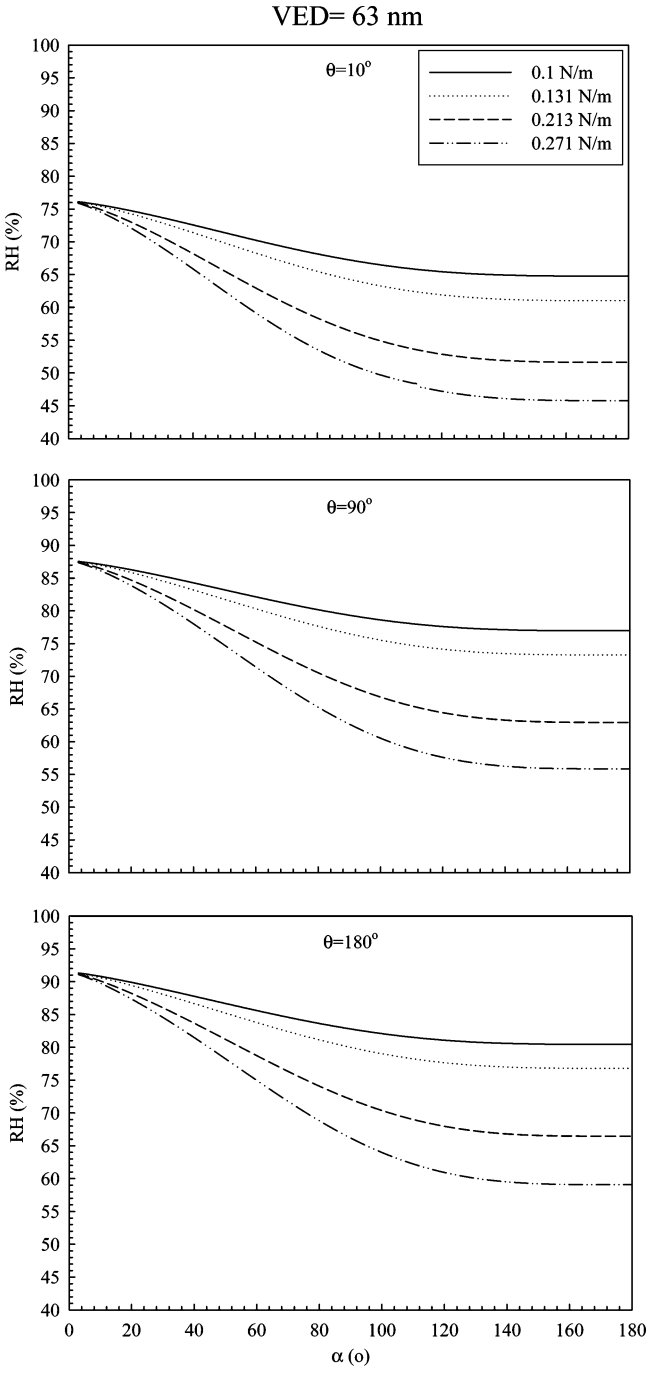

Figure 3. σ^{CV} effect on DRH variation with α for deposited particles having a volume equivalent diameter (VED) of 63 nm at $\theta = 10°$, 90°, and 180°.

In the model of Mirabel et al.,[23] deliquescence occurs when the two states have an identical free energy. Following this criterion and assuming the solution is ideal, we arrive at

$$3\sigma^{LV}g - 3\sigma^{CV}v^{c}(^{2}/_{3})\left[\frac{2 - 3\cos\alpha + \cos^{3}\alpha}{2 - 3\cos\theta + \cos^{3}\theta}\right]^{1}/_{3}g^{1}/_{3}x_{2}{}^{2}/_{3} + x_{2}{}^{2}/_{3}\left[\frac{3}{\pi(2 - 3\cos\theta + \cos^{3}\theta)}\right]^{1}/_{3}g^{1}/_{3}KTn_{2}{}^{1}/_{3}\ln\left(\frac{x_2}{\bar{x}_2}\right) - 2\sigma^{LV}v_1(1 - x_2) = 0 \quad (10)$$

with

$$g = v_1 - (v_1 - v_2)x_2$$

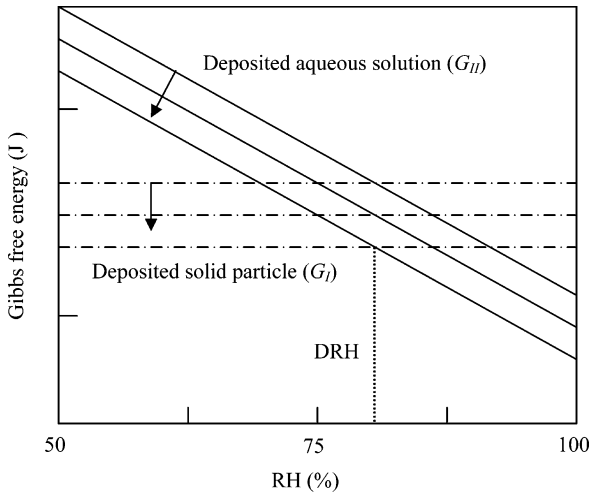

Figure 4. Sketch of variations of Gibbs free energies of a deposited solid particle and its aqueous solution with relative humidity.[25] The arrows indicate the directions of curve shift with decreasing contact angles, particle size or surface tension.

where x_2 is the molar fraction of solute in the droplet, $\bar{x}_2$ is the corresponding value in a bulk saturated solution, and σ^{LV} is a function of x_2. Note that when $\alpha = \theta = 180°$ eq 10 reduces to that for suspended particles. For a spherical cap of solution, one can easily modify the available derivation[32] to obtain the corresponding Köhler equation and calculate the relative humidity

$$RH = 100a_1 \exp\left(\frac{2\sigma^{LV}v_1}{kTR}\right) \quad (11)$$

where R is the curvature radius.

For deposited NaCl particles, we use $v_1 = 3.03 \times 10^{-29}$ m^3; $v_2 = 4.48 \times 10^{-29}$ m^3; $v^c = 4.48 \times 10^{-29}$ m^3. These parameters are calculated based on the corresponding densities and the solubility in water (35.9 g NaCl/100 mL water, i.e., $\bar{x}_2 = 0.0996$).[33] The surface tension, which depends on concentration, is given by[34]

$$\sigma^{LV} = 0.072 + 0.0017m \quad (12)$$

where m is the molality of NaCl. As for σ^{CV}, the available values reported in the literature cover a wide range, spanning from 0.09 to 0.348 N/m.[22−24] Mirabel et al.[23] chose four values (0.1, 0.112, 0.2, and 0.271 N/m) for their theoretical study, Russell and Ming[22] used 0.213 N/m, and Djikaev[24] deduced 0.348 N/m. The effect of σ^{CV} on DRH and how to obtain an effective value accounting for the initial water coating (a wetted particle)[22] will be discussed in detail in section 3.

After numerically solving eq 10 for x_2, we determine the water activity in the droplet and then the DRH from eq 11. When $m < 13$ mol/kg, the water activity in droplet solution is estimated by[35]

$$a_1 = \exp\left[-0.03604m + 0.01649(1 + 1.37m^{1}/^{2}) - (0.01649)(4.60517)\log(1 + 1.37m^{1}/^{2}) - \frac{0.01649}{(1 + 1.37m^{1}/^{2})} - 1.1601 \times 10^{-3}m^2 - 2.6572 \times 10^{-4}m^3 + 1.7029 \times 10^{-5}m^4\right] \quad (13)$$

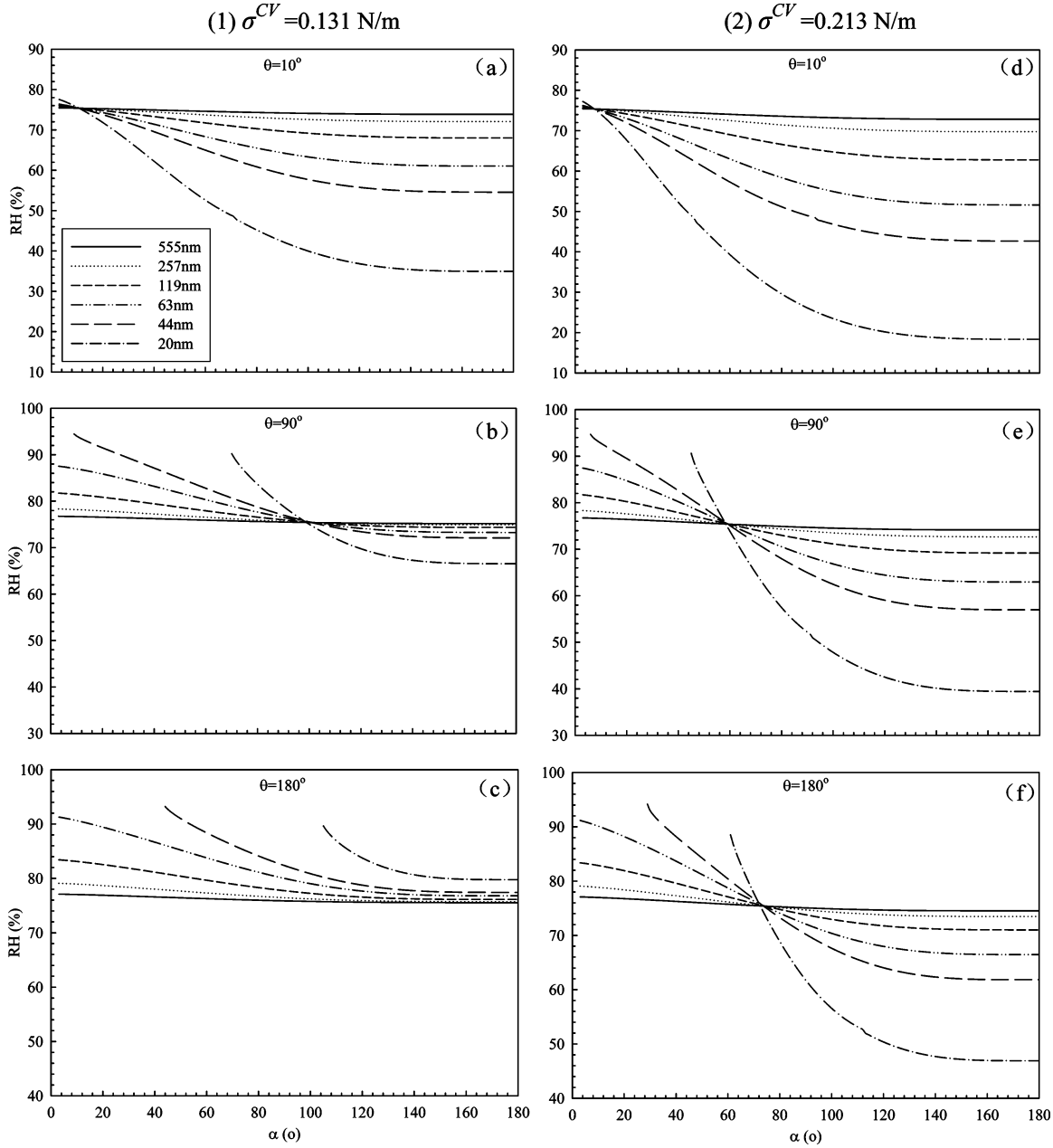

Figure 5. DRH of a deposited particle as a function of α with $\sigma^{CV} = 0.131$ and 0.213 N/m and at $\theta = 10^o$, 90^o, and 180^o.

Otherwise, the following formula is used:[36]

$$a_1 = (W - X)/W \tag{14}$$

where W represents the water moles in the solution and X is the amount of adsorbed water satisfying

$$X^2/[(qB - X)(W - X)] = \exp(-\epsilon_A/kT) = c_A \tag{15}$$

where B represents the salt moles in the solution, q is the number of adsorption sites per mole of the salt, and ϵ_A is the internal energy for a monolayer of water adsorbed onto the salt. The positive solution to the quadratic eq 15 gives the physically correct X value. For NaCl solution, Ally[36] reported $c_A = 3.813 \pm 0.2598$ and $q = 2.845 \pm 0.332$.

In the present formulation, we find that, at a given temperature, x_2 can be affected by α, θ, σ^{CV}, and n_2, so can DRH. We present and discuss the results for the individual effects in the following section, where the size of a dry particle represents the volume-equivalent diameter (VED).

3. Results and Discussions

Predicted DRH for suspended particles is quite sensitive to σ^{CV}, in particular for small particles.[23] As discussed in section 2, the reported values of σ^{CV} for NaCl span a considerable range. To investigate its effect, we plot in Figure 2 the calculated DRH against particle size for suspended particles ($\alpha = \theta = 180°$) for several values of σ^{CV} and make comparison with available experimental data. For suspended NaCl nanoparticles, Hämeri et al.[21] and Biskos et al.[10] systematically investigated the particle-size dependence of DRH using an ultrafine-DMA and tandem nano-DMAs. Note that the filled and open circles shown in Figure 2 are the experimental data of Biskos et al. for particles generated by a vaporization−condensation method and an electrospray technique, respectively. The experimental data reveal that DRH decreases with increasing particle size, and can be expressed by an empirical equation: $\mathrm{DRH}(D_m) = 213D_m^{-1.6} + 76$ with D_m being the dry particle mobility diameter (nm) for 6 nm $\le D_m \le$ 60 nm.[10] Also included in the figure is DRH calculated by the wetted particle model using $\sigma^{LC} = 0.029$

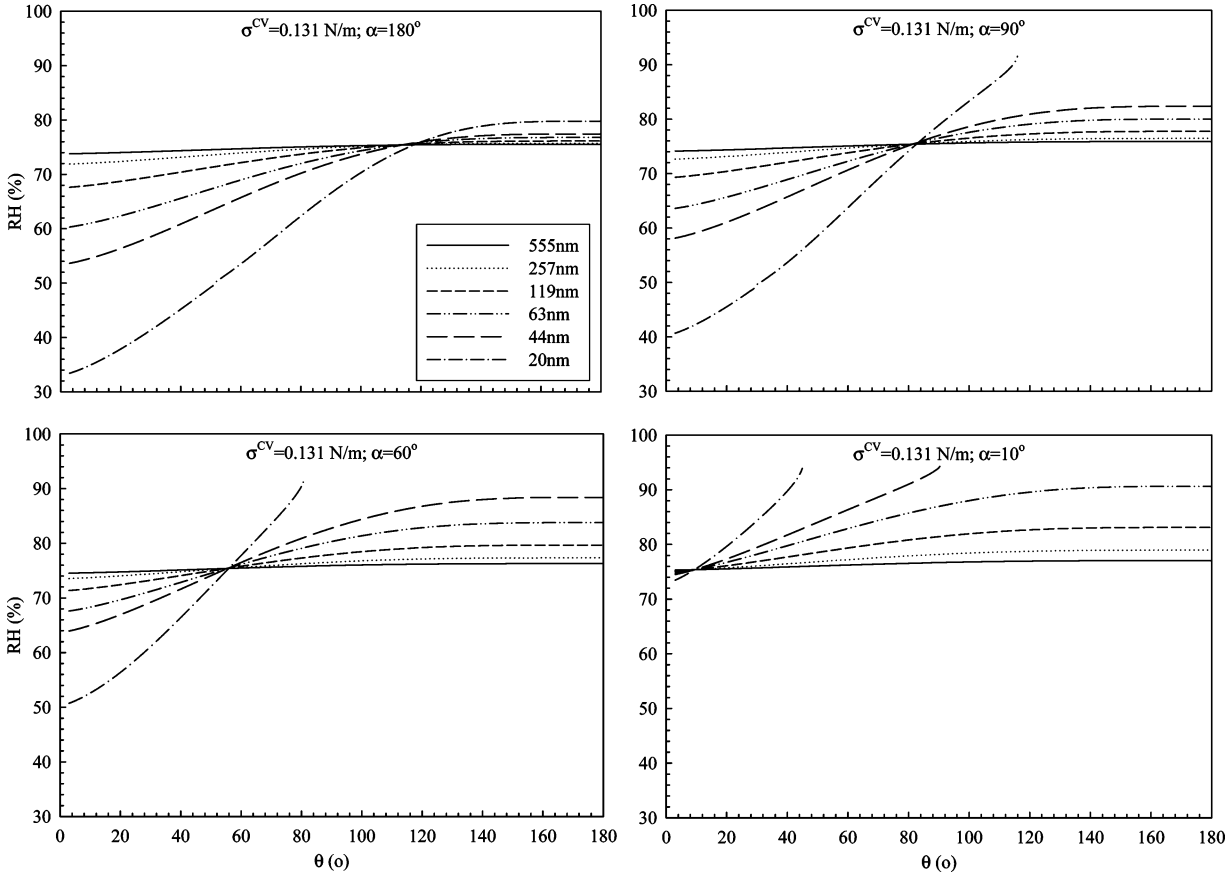

Figure 6. Variation of DRH with θ for different particle sizes at $\alpha = 180°$, 90°, 60°, and 10°.

N/m, $\sigma^{LV} = 0.083$ N/m, and the measured partial molar volume (line 6 of Figure 3 in ref 22), showing a good agreement with experiment. Interestingly, our theoretical prediction with $\sigma^{CV} = 0.131$ N/m compares favorably with the experimental data, too, except for $D_m < 8.6$ nm. The above comparison implies that 0.131 N/m can be regarded as an effective surface tension accounting for the initial water coating, although the formulation is based on a dry particle. It can be understood by comparing the free energies of the two initial states for a suspended particle; $\sigma^{CV}a^{CV}$ in the dry state will be replaced by $\sigma^{LV}a^{LV} + \sigma^{LC}a^{LC} + n_1^L\mu_1^L$ in the coated state. When the water layer is comparatively thin enough (i.e., small n_1^L and $a^{LV} \approx a^{LC} \approx a^{CV}$), the change of chemical potential for n_1^L water molecules after deliquescence has a negligible effect on the DRH calculation. This can also explain why our prediction worsens for $D < 8$ nm. We therefore employ $\sigma^{CV} = 0.131$ N/m to calculate DRH for most of the cases, where the NaCl particles are greater than 8.6 nm. Note that for sufficiently large particles DRH is only weakly affected by σ^{CV}, although the results are not shown in Figure 2.

Figure 3 shows DRH as a function of α at various θ for particles with VED of 63 nm. The calculated DRH is lower for larger σ^{CV}, similar to that of suspended particles,[23] and increases with decreasing α. In fact, when α approaches zero, DRH converges to the same value, independent of σ^{CV}. The weaker σ^{CV} effect at smaller α can be understood as follows. Using eqs 4-6, eq 1 can be rewritten as

$$G_I = N\mu_1^v + n_2\mu_2^c + \pi\left(\frac{3n_2v^c}{\pi}\right)^{2/3}\sigma^{CV}(2 - 3\cos\alpha + \cos^3\alpha)^{1/3} + \sigma^{SV}S \quad (16)$$

Note that the third term on the right-hand side of eq 16 represents the surface energy change (mechanical work) after the particle is deposited. When α decreases, this term decreases and actually vanishes at $\alpha = 0$, where the free energy becomes unaffected by σ^{CV}. From eq 16, we also find that the relative magnitude of chemical to mechanical work (i.e., the ratio of the second to third term) is proportional to $n_2^{1/3}$, indicative of increasing importance of the mechanical work when the particle decreases in size.

Figure 4 sketches how the free energies for a solid particle and a corresponding solution droplet vary with RH.[25] At low RH, the free energy of solid particle is lower than that of the corresponding solution droplet, so the dry particle remains thermodynamically stable. When RH increases, the free energy of the solution droplet decreases and becomes equal to that of the solid particle at a certain RH, which is regarded as DRH in the present study. As RH further increases, the free energy of the solution droplet is lower than that of the dry state, and thereby the solid particle spontaneously absorbs water to form a solution droplet.[25] An increase in σ^{CV} or α means an upward shift of the dash-dotted line (G_I) in Figure 4, leading to a crossover at a lower RH.

Figure 5 plots DRH as a function of α for six particle sizes ranging from 20 to 555 nm for two values of σ^{CV}: 0.131 and 0.231 N/m. Only for small particles does the variation in α substantially influence DRH; when the particle size is larger than 555 nm, α hardly affects DRH. At a given σ^{CV}, DRH may exhibit opposite trends with varying particle size, depending on both α and θ (see Figure 5). The crossover region appears to shift toward a greater value of α when θ is increased and may disappear for certain cases, such as that shown in Figure 5c. The complicated behavior can be explained by how the free

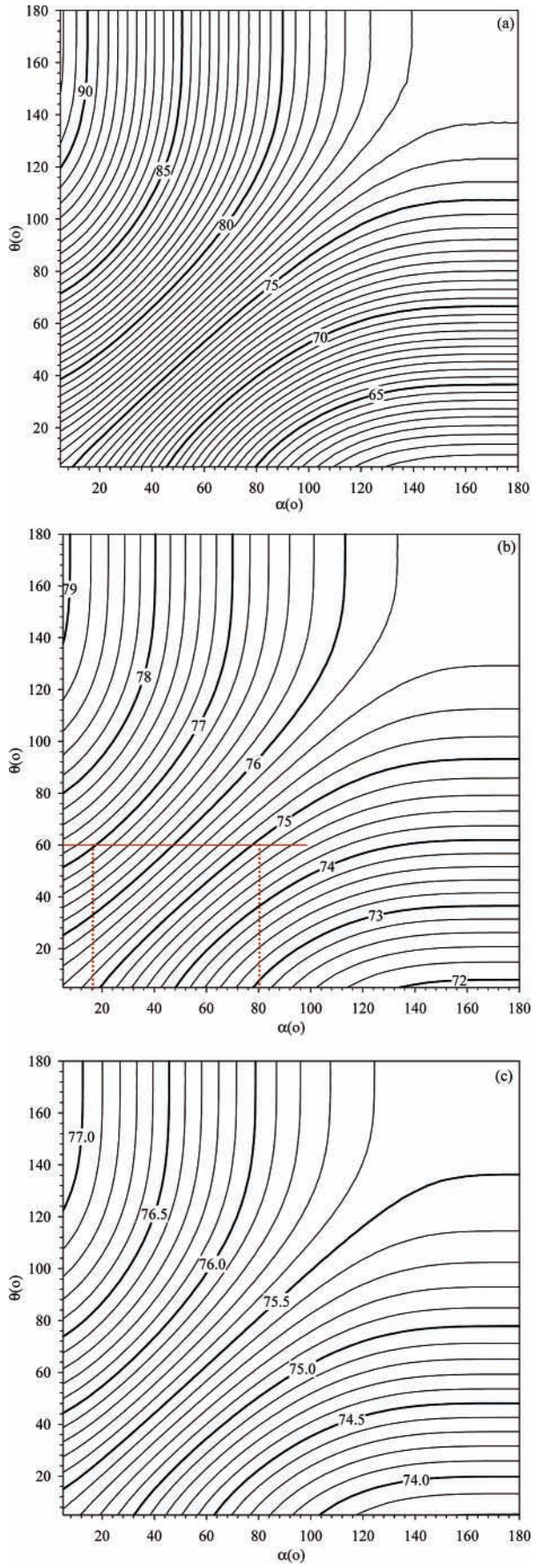

Figure 7. Contour plots for DRH as a function of the contact angles (α and θ) for deposited NaCl particles with dry diameter: $D = 63$ (a), 257 (b), and 555 nm (c). The value for each curve denotes the DRH in %.

energies change when the particle size is varied. Depending on α, θ, and σ^{CV}, both G_I and G_{II} (eqs 1 and 2) decrease with decreasing particle size, but at different rates, leading to a complex trend in the crossover shift shown in Figure 4.

The variation of DRH with θ is presented in Figure 6 for $\sigma^{CV} = 0.131$ N/m, where one can again see a significant effect only for small particles. A decrease in θ lowers the free energy of the droplet as demonstrated by the rearranged eq 2

$$G_{II} = (N - n_1)\mu_1^v + n_2\mu_2 + n_1\mu_1 + \pi\left[\frac{3(n_1\upsilon_1 + n_2\upsilon_2)}{\pi}\right]^{2}/^{3}\sigma^{LV}(2 - 3\cos\theta + \cos^3\theta)^{1}/^{3} + \sigma^{SV}S \quad (17)$$

leading to a lower DRH which can be visualized in Figure 4. For larger particles, because the chemical potential terms dominate over the influence of surface tension (the fourth term of eq 17), the effect of θ on the DRH becomes weaker. In addition, Figure 6 shows that the location of the crossover region with respect to θ depends on the α value, which can also be understood from the different change rates of G_I and G_{II} as particles vary in size. From Figures 5 and 6, one can find that for sufficiently small particles, the DRH could be substantially lowered when θ is small, but α is not small. It corresponds to a case where small particles in a nearly spherical shape are deposited on a hydrophilic substrate. This finding suggests that corrosion associated with deliquescent deposited aerosol may take place at a rather low RH.

To the best of our knowledge, there exist only two experimental works examining the DRH of deposited particles (100 nm to 20 μm) with the results shown in Table 1. Verifying our theoretical prediction requires the interfacial properties in terms of α, θ, and σ^{CV} measured experimentally along with the DRH, which unfortunately could not be provided by these two studies using environmental-TEM or environmental-SEM. To roughly estimate the range of α, one can use the DRH contour plots shown in Figure 7. For instance, using the measured $\theta = 60°$ for a large NaCl solution drop on a TEM grid, the α range is found to be 16°∼80° for $D = 257$ nm from the data in Table 1 and Figure 7b.

Finally, we briefly review and suggest feasible laboratory experiments to measure the contact angles, and interfacial properties of nanosized particles on substrates. To determine the contact angles of deposited dry and wet particles, in situ measurements using tapping-mode AFM appears to be one of the most promising techniques, because of its strength of providing three-dimensional images, in particular for a contact angle smaller than 90°.[37−41] Wang et al.[39,40] reported the contact angles of 10.8° and 22° for nanosized water droplets on mica and stainless steel (SUS 304), respectively. They also found that the contact angels appear to decrease with decreasing particle sizes, which is consistent with the observations of micron-sized droplets.[42] Because the surface properties of a substrate can affect the contact angles,[40,43−45] one should take into account the composition, roughness, homogeneity, and preparation method for the substrate surface when designing experiments. For instance, the contact angle of a water droplet on Formvar (a kind of coating on a TEM grid) can vary from 50° to 83°,[34,44] whereas it can become as small as 35° if a carbon film is used as the substrate.[46] In addition, since the methods of depositing particles on a substrate may also affect the interfacial properties (contact angle and surface tension),[45] a consistent experimental preparation and execution is important to obtain reproducible data.

4. Conclusions

The model of Mirabel et al.[23] has been extended to study the deliquescence of particles deposited on a substrate. To facilitate the formulation and calculation, we have assumed that the particle, dry or wet, is in a shape of spherical cap. For deposited particles smaller than 100 nm, the DRH substantially depends on the particle size, the contact angles, and the surface tension between the dry particle and the atmosphere, whereas the substrate effect is insignificant for large particles (>500 nm). Depending on the contact angles, small particles depositing on a substrate could deliquesce at a much lower RH, posing a potential corrosion problem for the substrate. Although our formulation is based on spherical caps, it can be easily modified to investigate a deposited particle with experimentally measured shape, dimensions and σ^{CS}. In the future, more experimental investigation providing the shape or contact angles in parallel with corresponding DRH for deposited particles smaller than 100 nm is needed to verify the present theoretical understanding of the deliquescent behavior.

Acknowledgment. The authors are grateful to the financial support from National University of Singapore through Grants R-279-000-172-112 and R-279-000-144-112.

References and Notes

(1) Xu, J.; Imre, D.; McGraw, R.; Tang, I. *J. Phys. Chem. B* **1998**, *102*, 7462−7469.
(2) Lightstone, J. M.; Onasch, T. B.; Imre, D. *J. Phys. Chem. A* **2000**, *104*, 9337−9346.
(3) Cruz, C. N.; Pandis, S. N. *Environ. Sci. Technol.* **2000**, *34*, 4313−4319.
(4) Martin, S. T.; Schlenker, J.; Chelf, J. H.; Duckworth, O. W. *Environ. Sci. Technol.* **2001**, *35*, 1624−1629.
(5) Tang, I. N.; Munkelwitz, H. R.; Davis, J. G. *J. Aerosol. Sci.* **1978**, *9*, 505−511.
(6) Shulman, M. L.; Charlson, R. J.; Davis, E. J. *J. Aerosol. Sci.* **1997**, *28*, 737−752.
(7) Hämeri, K.; Väkevä, M.; Hansson H. C.; Laaksonen, A. *J. Geophys. Res.* **2000**, *105*, 22231−22242.
(8) Choi, M. Y.; Chan, C. K. *Environ. Sci. Technol.* **2002**, *36*, 2422−2428.
(9) Gysel, M.; Weingartner, E.; Baltensperger, U. *Environ. Sci. Technol.* **2002**, *36*, 63−68.
(10) Biskos, G.; Malinowski, A.; Russell, L. M.; Buseck, P. R.; Martin, S. T. *Aerosol Sci. Technol.* **2006**, *40*, 97−106.
(11) Sinclair, J. D.; Psota-Kelty, L. A.; Weschler, C. J. Shields, H. C. *J. Electrochem. Soc.* **1990**, *137*, 1200−1206.
(12) Frankenthal, R. P.; Siconolfi, D. J.; Sinclair, J. D. *J. Electrochem. Soc.* **1993**, *140*, 3129−3134.
(13) Litvak, A.; Gadgil, A. J.; Fisk, W. *Indoor Air* **2000**, *10*, 47−56.
(14) Zhang, J.; Wang, J.; Wang, Y. *Corrosion* **2005**, *61*, 1167−1172.
(15) Baboian, R.; Hopkins, A. G.; Kane, R. D.; Kelly, R. C.; Buck, E. *Corrosion Tests and Standards: Application and Interpretation*; ASTM: USA, 2000; Chapter 70.
(16) Ebert, M.; Marion, I. H.; Weinbruch, S. *Atmos. Environ.* **2002**, *36*, 5909−5916.
(17) Wise, M. E.; Biskos, G.; Martin, S. T.; Russell, L. M.; Buseck, P. R. *Aerosol Sci. Technol.* **2005**, *39*, 849−856.
(18) Tang, I. N.; Munkelwitz, H. R. *J. Colloid Interf. Sci.* **1984**, *98*, 430−438.
(19) Cohen, M. D.; Flagan, R. C.; Seinfeld, J. H. *J. Phys. Chem.* **1987**, *91*, 4563−4574.
(20) Cziczo, D. J.; Nowak, J. B.; Hu, J. H.; Abbatt, J. P. D. *J. Geophys. Res.* **1997**, *102*, 18843−18850.
(21) Hämeri, K.; Laaksonen, A.; Väkevä, M.; Suni, T. *J. Geophys. Res.* **2001**, *106*, 20749−20757.
(22) Russell, L. M.; Ming, Y. *J. Chem. Phys.* **2002**, *116*, 311−321.
(23) Mirabel, P.; Reiss, H.; Bowles, R. K. *J. Chem. Phys.* **2000**, *113*, 8200−8205.
(24) Djikaev, Y. S.; Bowles, R.; Reiss, H.; Hämeri, K.; Laaksonen, A.; Vakeva, M. *J. Phys. Chem. B* **2001**, *105*, 7708−7722.
(25) Defay, R.; Prigogine, I.; Bellemans, A.; Everett, D. H. *Surface Tension and Adsorption*; Longmans, Green & Co Ltd: London, 1966; pp 287−309.
(26) Mutaftschiev, B. *The Atomistic Nature of Crystal Growth*; Springer-Verlag: New York, 2001; pp 147−161.
(27) Richardson, C. B.; Snyder, T. D. *Langmuir* **1994**, *10*, 2462−2465.
(28) Onasch, T. B.; McGraw, R.; Imre, D. *J. Phys. Chem. A* **2000**, *104*, 10797−10806.
(29) Han, J. H.; Hung, H. M.; Martin, S. T. *J. Geophys. Res.* **2002**, *107*, 4086.
(30) Liu, X. Y. *J. Cryst. Growth* **2002**, *237*−239, 1806−1812.
(31) Mirabel, P.; Reiss, H.; Bowles, R. K. *J. Chem. Phys.* **2000**, *113*, 8194−8199.
(32) Seinfeld, J. H.; Pandis, S. N. *Atmospheric Chemistry and Physics: From Air Pollution to Climate Change*; John Wiley: New York, 1998; pp 507−751.
(33) Lide, D. R., Ed.; *CRC Handbook of Chemistry and Physics*; Taylor and Francis: Boca Raton, FL, 2006; Internet Version, http://www.hbcpnetbase.com.
(34) Pruppacher, H. R.; Klett, J. D. *Microphysics of clouds and precipitation*; D. Reidel: Dordrecht, Holland, 1978; pp 100−109.
(35) Tang, I. N.; Munkelwitz, H. R.; Wang, N. *J. Colloid Interf. Sci.* **1986**, *114*, 409−415.
(36) Ally, M. R.; Clegg, S. L.; Braunstein, J.; Simonson, J. M. *J. Chem. Thermodynamics* **2001**, *33*, 905−915.
(37) Herminghaus, S.; Fery, A.; Reim, D. *Ultramicroscopy* **1997**, *69*, 211−217.
(38) Pompe, T.; Fery, A.; Herminghaus, S. *Langmuir* **1998**, *14*, 2585−2588.
(39) Wang, R.; Takeda, M.; Kido, M. *Mater. Lett.* **2002**, *54*, 140−144.
(40) Wang, R.; Cong, L.; Kido, M. *Appl. Surf. Sci.* **2002**, *191*, 74−84.
(41) Wang, R.; Kido, M. *Surf. Interface Anal.* **2005**, *37*, 1105−1110.
(42) Ueda, S.; Shi, H.; Jiang, X.; Shibata, H.; Cramb, A. W. *Metall. Mater. Trans. B* **2003**, *34*, 503−508.
(43) Ponsonnet, L.; Reybier, K.; Jaffrezic, N.; Comte, V.; Lagneau, C.; Lissac, M.; Martelet, C. *Mater. Sci. Eng. C* **2003**, *23*, 551−560.
(44) Hennig, A.; Eichhorn, K. J.; Staudinger, U.; Sahre, K.; Rogalli, M.; Stamm, M.; Neumann, A. W.; Grundke, K. *Langmuir* **2004**, *20*, 6685−6691.
(45) Adamson, A. W.; Gast, A. P. *Physical Chemistry of Surfaces*; Wiley: New York, 1997.
(46) Mattia, D.; Bau, H. H.; Gogotsi, Y. *Langmuir* **2006**, *22*, 1789−1794.